

Association of peripheral blood pressure with gray matter volume in 19- to 40-year-old adults

H. Lina Schaare, MSc, Shahrzad Kharabian Masouleh, MSc, Frauke Beyer, MSc, Deniz Kumral, MSc, Marie Uhlig, MSc, Janis D. Reinelt, Andrea M.F. Reiter, PhD, Leonie Lampe, MD, Anahit Babayan, PhD, Miray Erbey, MSc, Josefin Roebbig, MSc, Matthias L. Schroeter, MD, PhD, Hadas Okon-Singer, PhD, Karsten Müller, PhD, Natacha Mendes, PhD, Daniel S. Margulies, PhD, A. Veronica Witte, PhD, Michael Gaebler, PhD, and Arno Villringer, MD

Correspondence

H.L. Schaare
schaare@cbs.mpg.de

Neurology® 2019;92:e1-e16. doi:10.1212/WNL.0000000000006947

Abstract

Objective

To test whether elevated blood pressure (BP) relates to gray matter (GM) volume (GMV) changes in young adults who had not previously been diagnosed with hypertension (systolic BP [SBP]/diastolic BP [DBP] $\geq 140/90$ mm Hg).

Methods

We associated BP with GMV from structural 3T T1-weighted MRI of 423 healthy adults between 19 and 40 years of age (mean age 27.7 ± 5.3 years, 177 women, SBP/DBP $123.2/73.4 \pm 12.2/8.5$ mm Hg). Data originated from 4 previously unpublished cross-sectional studies conducted in Leipzig, Germany. We performed voxel-based morphometry on each study separately and combined results in image-based meta-analyses (IBMA) to assess cumulative effects across studies. Resting BP was assigned to 1 of 4 categories: (1) SBP <120 and DBP <80 mm Hg, (2) SBP 120–129 or DBP 80–84 mm Hg, (3) SBP 130–139 or DBP 85–89 mm Hg, (4) SBP ≥ 140 or DBP ≥ 90 mm Hg.

Results

IBMA yielded the following results: (1) lower regional GMV was correlated with higher peripheral BP; (2) lower GMV was found with higher BP when comparing individuals in subhypertensive categories 3 and 2, respectively, to those in category 1; (3) lower BP-related GMV was found in regions including hippocampus, amygdala, thalamus, frontal, and parietal structures (e.g., precuneus).

Conclusion

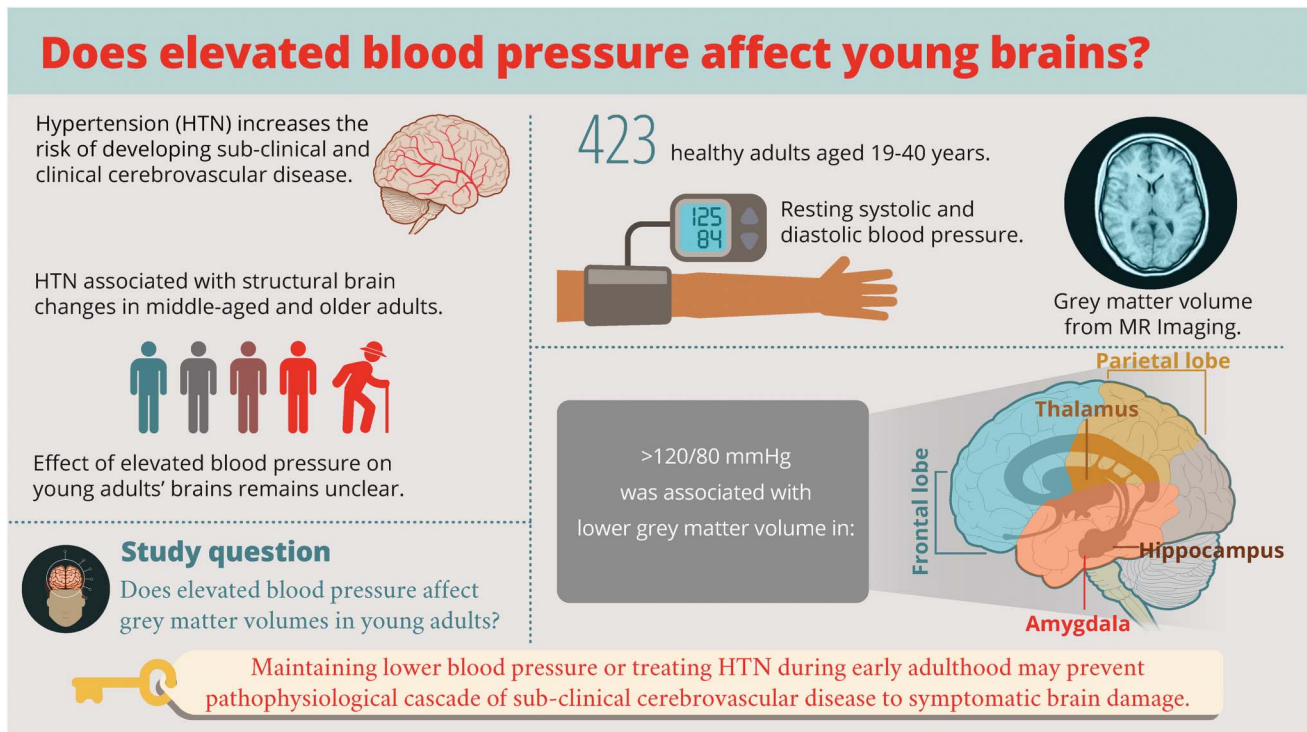
BP $\geq 120/80$ mm Hg was associated with lower GMV in regions that have previously been related to GM decline in older individuals with manifest hypertension. Our study shows that BP-associated GM alterations emerge continuously across the range of BP and earlier in adulthood than previously assumed. This suggests that treating hypertension or maintaining lower BP in early adulthood might be essential for preventing the pathophysiologic cascade of asymptomatic cerebrovascular disease to symptomatic end-organ damage, such as stroke or dementia.

From the Department of Neurology (H.L.S., S.K.M., F.B., D.K., M.U., J.D.R., A.M.F.R., L.L., A.B., M.E., J.R., M.L.S., A.V.W., M.G., A.V.), Max Planck Research Group for Neuroanatomy & Connectivity (N.M., D.S.M.), and Nuclear Magnetic Resonance Group (K.M.), Max Planck Institute for Human Cognitive and Brain Sciences; International Max Planck Research School NeuroCom (H.L.S., M.U.), Leipzig; MindBrainBody Institute at Berlin School of Mind and Brain (D.K., A.B., M.E., M.G., A.V.), Charité & Humboldt Universität zu Berlin; Lifespan Developmental Neuroscience (A.M.F.R.), Technische Universität Dresden; Leipzig Research Centre for Civilization Diseases (LIFE) (M.L.S., M.G., A.V.), Clinic for Cognitive Neurology (M.L.S., A.V.), and Collaborative Research Centre 1052 'Obesity Mechanisms,' Subproject A1, Faculty of Medicine (F.B., A.V.W., A.V.), University of Leipzig, Germany; Department of Psychology (H.O.-S.), University of Haifa, Israel; and Center for Stroke Research Berlin (A.V.), Charité-Universitätsmedizin Berlin, Germany.

Go to [Neurology.org/N](https://www.neurology.org/N) for full disclosures. Funding information and disclosures deemed relevant by the authors, if any, are provided at the end of the article.

Glossary

AD = Alzheimer disease; ANOVA = analysis of variance; BMI = body mass index; BP = blood pressure; CSFV = cerebrospinal fluid volume; CVD = cerebrovascular disease; DBP = diastolic blood pressure; FA = flip angle; FLAIR = fluid-attenuated inversion recovery; FOV = field of view; FWE = family-wise error; GM = gray matter; GMV = gray matter volume; HTN = hypertension; IBMA = image-based meta-analyses; LIFE Study = Leipzig Research Centre for Civilization Diseases Study; ROI = region of interest; SBP = systolic blood pressure; SDM = seed-based *d* mapping; TE = echo time; TI = inversion time; TIV = total intracranial volume; TR = repetition time; VBM = voxel-based morphometry; WM = white matter; WMH = white matter hyperintensities; WMV = white matter volume.



NPub.org/875914

doi: 10.1212/WNL.000000000000694

Copyright © 2019 American Academy of Neurology

Neurology®

Hypertension (HTN) is highly prevalent and the leading single risk factor for global disease burden and overall health loss.^{1,2} The risk for insidious brain damage and symptomatic cerebrovascular disease (CVD) (e.g., stroke and vascular dementia) multiplies with manifestation of HTN.³ Midlife HTN is a major risk factor for late-life cognitive decline and has been associated with risk for dementia, including late-onset Alzheimer disease (AD).³⁻⁵

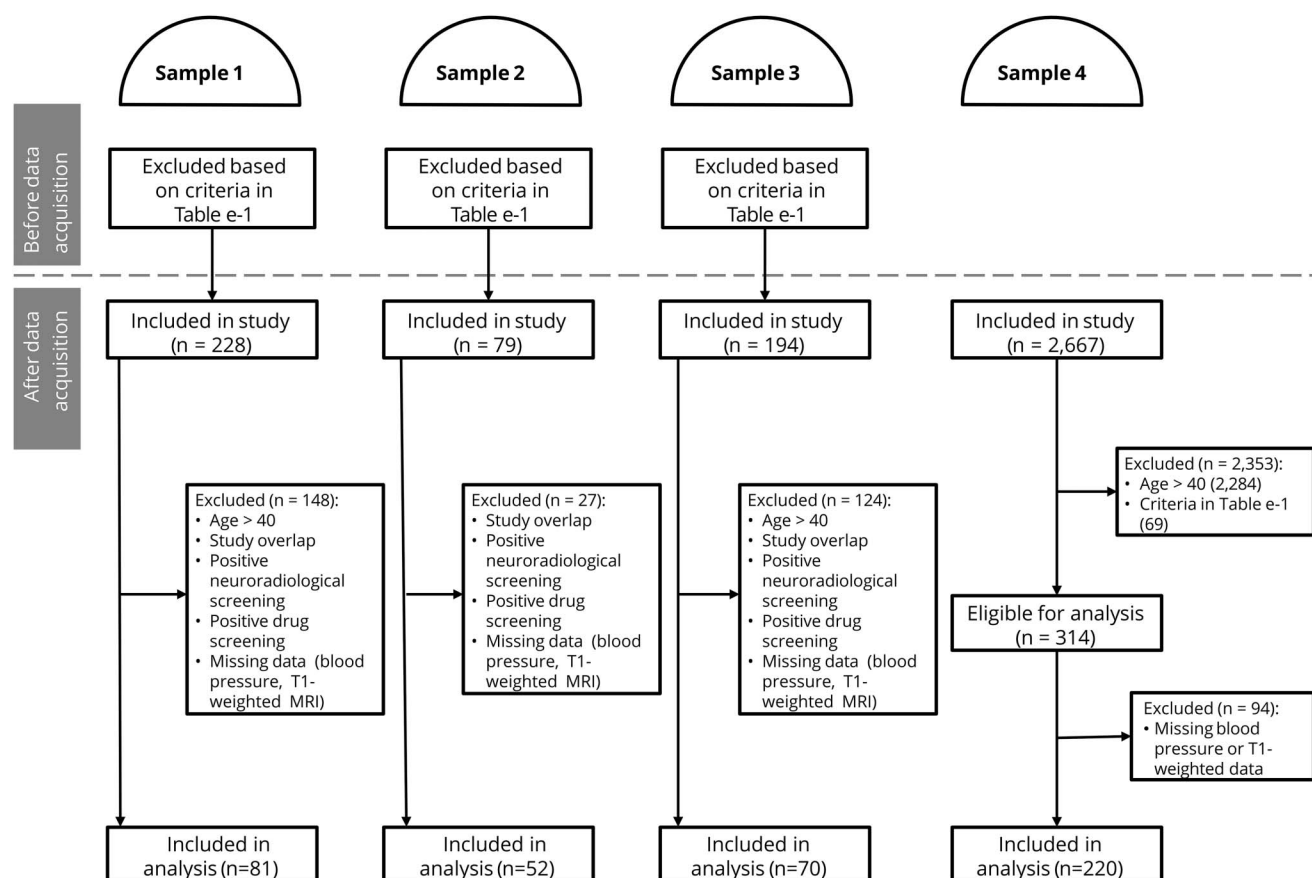
Importantly, HTN is also related to subclinical functional^{6,7} and structural⁵⁻¹⁴ brain changes, or asymptomatic CVD, including brain volume reductions in the medial temporal and frontal lobes.^{5,6,9-11,15} Hippocampal volumes, in particular, have been consistently associated with HTN-related reductions.^{5,9,10,15} Furthermore, computational anatomy has been employed to detect subtle cerebral changes, such as microstructural white matter (WM) alterations¹³ or reductions in regional gray matter

(GM),^{5,11} in middle-aged and older adults with elevated blood pressure (BP).

Recent statements suggest that symptomatic clinical disease, resulting from elevated BP, could be prevented by avoiding primary BP elevations and subclinical target organ damage (including brain damage) in early adulthood and middle age.^{3,16,17} However, effects of elevated BP on adult brains before the age of 40 are unclear. Preliminary evidence from 32 young, normotensive adults showed that BP reactivity correlated with lower amygdala volume.¹⁸

This study aimed to investigate if subtle structural brain changes occur in early adulthood (<40 years) at sub-hypertensive BP levels. We hypothesized that higher BP would relate to lower regional GM volume (GMV) and that this would predominantly affect frontal and medial temporal lobes, including amygdala and hippocampus.

Figure 1 Flow chart with inclusion procedure for the 4 samples



Sample 1: Leipzig Study for Mind–Body–Emotion Interactions. Sample 2: Neural Consequences of Stress Study. Sample 3: Neuroanatomy and Connectivity Protocol. Sample 4: Leipzig Research Centre for Civilization Diseases (MRI subcohort).

Methods

We applied voxel-based morphometry^{19,20} (VBM) to 4 previously unpublished independent datasets including young adults aged between 19 and 40 years without previous diagnosis of HTN or any other severe, chronic, or acute disease. Results from each dataset were combined in image-based meta-analyses (IBMA) for well-powered, cumulative evaluation of findings across study differences (i.e., recruitment procedure, inclusion criteria, and data acquisition, figure 1 and table e-1, doi.org/10.1101/239160).

Participants

We included cross-sectional data of 423 young participants from 4 samples. The samples were drawn from larger studies that were conducted in Leipzig, Germany, between 2010 and 2015: (1) Leipzig Study for Mind–Body–Emotion Interactions (Babayan et al., under review), (2) Neural Consequences of Stress Study (Reinelt et al., in preparation), (3) Neuroanatomy and Connectivity Protocol,²¹ and (4) Leipzig Research Centre for Civilization Diseases Study (LIFE Study).²²

The objective of study 1 was to cross-sectionally investigate mind–brain–body–emotion interactions in a younger (20–35 years) and an older (59–77 years) group of 228 healthy volunteers. Study 2 aimed to investigate neural correlates of acute psychosocial stress in 79 young (18–35 years), healthy, non-smoking men. The study protocol for the baseline assessment of participants in study 2 was adapted from the protocol in study 1. In study 3, 194 healthy volunteers between 20 and 75 years of age participated in 1 session of MRI and completed an extensive assessment of cognitive and personality measures. This dataset aimed to relate intrinsic functional brain connectivity with cognitive faculties, self-generated mental experience, and personality features. Together, studies 1–3 constitute the MPI-Leipzig Mind–Brain–Body database. Study 4 (LIFE Study) is a population-based dataset in Leipzig, Germany, with the objective to investigate the development of major modern diseases. Overall, 10,000 participants were randomly drawn from the local population, of whom 2,667 underwent MRI and detailed screening. With dementia being one of the key scientific topics in this study, most participants in the MRI subcohort were adults older than 60 years. The exact inclusion procedure and numbers for the current investigation are

Table 1 Characteristics by blood pressure (BP) category

| | Total | Category 1 | Category 2 | Category 3 | Category 4 | <i>p</i> Value | Pairwise comparisons |
|--|-------------------|-------------------|-------------------|-------------------|-------------------|----------------|--|
| No. (%) | 423 (100) | 175 (41) | 121 (29) | 80 (19) | 47 (11) | | |
| Women, n (%) | 177 (42) | 117 (67) | 40 (33) | 11 (14) | 9 (19) | ^a | 2, ^a 3, ^a 4 ^a |
| Age, y, mean (SD) | 27.66 (5.27) | 27.61 (5.53) | 27.30 (4.95) | 28.01 (5.24) | 28.21 (5.23) | | |
| Range, y, min-max | 19–40 | 19–40 | 20–40 | 20–40 | 20–39 | | |
| SBP, mm Hg, mean (SD) | 123.2 (12.19) | 111.91 (5.44) | 123.99 (3.62) | 134.57 (3.48) | 143.56 (7.76) | ^a | 2 ^a 3, ^a 4 ^a |
| DBP, mm Hg, mean (SD) | 73.38 (8.49) | 67.67 (5.81) | 73.64 (5.77) | 78.79 (6.46) | 84.75 (8.26) | ^a | 2, ^a 3, ^a 4 ^a |
| Body mass index, kg/m ² , mean (SD) | 23.48 (3.25) | 22.60 (2.74) | 23.45 (3.23) | 24.22 (3.42) | 25.59 (3.62) | ^a | 2, ^b 3, ^c 4 ^a |
| Missing values, n (%) | 13 (3) | 5 (3) | 4 (3) | 1 (1) | 3 (6) | | |
| Range, kg/m ² , min-max | 17.96–36.93 | | | | | | |
| Smoking status, n (%) | | | | | | | |
| Nonsmoker | 273 (65) | 113 (65) | 78 (64) | 53 (66) | 29 (62) | | |
| Occasional smoker | 57 (13) | 23 (13) | 17 (14) | 13 (16) | 4 (9) | | |
| Smoker | 73 (17) | 29 (17) | 21 (17) | 13 (16) | 10 (21) | | |
| Missing values | 20 (5) | 10 (6) | 5 (4) | 1 (1) | 4 (9) | | |
| Fazekas score, n (%) | | | | | | | |
| 0 | 303 (72) | 123 (70) | 85 (70) | 59 (74) | 36 (77) | | |
| 1 | 72 (17) | 39 (22) | 16 (13) | 10 (13) | 7 (15) | | |
| 2 | 0 (0) | 0 (0) | 0 (0) | 0 (0) | 0 (0) | | |
| 3 | 0 (0) | 0 (0) | 0 (0) | 0 (0) | 0 (0) | | |
| Missing values | 48 (11) | 13 (7) | 20 (17) | 11 (14) | 4 (9) | | |
| Total intracranial volume, mL, mean (SD) | 1,450.05 (137.39) | 1,400.49 (127.47) | 1,457.43 (142.07) | 1,508.05 (116.23) | 1,516.90 (126.29) | | |
| Gray matter volume, mL, mean (SD) | 777.41 (88.69) | 748.55 (79.50) | 784.29 (90.41) | 809.72 (87.36) | 812.16 (86.47) | | |
| White matter volume, mL, mean (SD) | 449.79 (55.74) | 435.84 (53.56) | 452.75 (55.93) | 464.19 (53.34) | 469.58 (55.52) | | |
| CSF volume, mL, mean (SD) | 222.86 (56.60) | 216.09 (54.57) | 220.40 (59.53) | 234.14 (54.14) | 235.16 (57.34) | | |
| Hippocampal volume, left, mL, mean (SD) | 3.90 (0.45) | 3.77 (0.41) | 3.93 (0.46) | 4.06 (0.43) | 4.09 (0.43) | | |
| Hippocampal volume, right, mL, mean (SD) | 3.97 (0.43) | 3.83 (0.40) | 4.00 (0.44) | 4.12 (0.40) | 4.14 (0.39) | | |
| Amygdalar volume, left, mL, mean (SD) | 1.68 (0.19) | 1.62 (0.18) | 1.68 (0.19) | 1.75 (0.18) | 1.75 (0.18) | | |
| Amygdalar volume, right, mL, mean (SD) | 1.50 (0.16) | 1.45 (0.15) | 1.51 (0.17) | 1.56 (0.16) | 1.57 (0.15) | | |

Abbreviations: DBP = diastolic blood pressure; SBP = systolic blood pressure.

The *p* Value column specifies significant results of comparisons between BP categories: empty cells = *p* > 0.05.

The Pairwise comparisons column specifies significant post hoc comparisons for: 2 = category 1 vs 2, 3 = category 1 vs 3, 4 = category 1 vs 4. ^a *p* < 0.001; ^b *p* < 0.05; ^c *p* < 0.01.

Definition of BP categories: category 1, SBP <120 mm Hg and DBP <80 mm Hg; category 2, SBP 120–129 mm Hg or DBP 80–84 mm Hg; category 3, SBP 130–139 mm Hg or DBP 85–89 mm Hg; and category 4, SBP ≥140 mm Hg or DBP ≥90 mm Hg.

Table 2 Characteristics by sample

| | Total | Sample 1 | Sample 2 | Sample 3 | Sample 4 | p Value | Pairwise comparisons |
|---|-------------------|-------------------|-------------------|-------------------|-------------------|--------------|--|
| No. | 423 | 81 | 52 | 70 | 220 | | |
| Women, n (%) | 177 (42) | 37 (46) | 0 (0) | 43 (61) | 97 (44) | ^a | 1 vs 2, ^a 2 vs 3, ^a 2 vs 4, ^a 3 vs 4 ^b |
| Age, y, mean (SD) | 27.66 (5.27) | 24.36 (3.07) | 25.77 (2.44) | 26.54 (4.82) | 29.69 (5.65) | ^a | 1 vs 3, ^b 1 vs 4, ^a 2 vs 4, ^a 3 vs 4 ^a |
| Range, y, min-max | 19–40 | 20–35 | 21–31 | 20–40 | 19–40 | | |
| SBP, mm Hg, mean (SD) | 123.2 (12.19) | 121.8 (12.02) | 128.4 (9.80) | 128.4 (12.16) | 120.8 (11.95) | ^a | 1 vs 2, ^c 1 vs 3, ^a 2 vs 4, ^a 3 vs 4 ^a |
| DBP, mm Hg, mean (SD) | 73.38 (8.49) | 73.27 (6.77) | 75.68 (8.03) | 79.91 (7.65) | 70.80 (8.20) | ^a | 1 vs 3, ^a 1 vs 4, ^b 2 vs 3, ^c 2 vs 4, ^a 3 vs 4 ^a |
| BP category, n (%) | | | | | | ^a | 1 vs 2, ^b 1 vs 3, ^c 2 vs 4, ^a 3 vs 4 ^a |
| Category 1 (SBP <120 mm Hg and DBP <80 mm Hg) | 175 (41) | 38 (47) | 10 (19) | 15 (21) | 112 (51) | | |
| Category 2 (SBP 120–129 mm Hg or DBP 80–84 mm Hg) | 121 (29) | 23 (28) | 21 (40) | 19 (27) | 58 (26) | | |
| Category 3 (SBP 130–139 mm Hg or DBP 85–89 mm Hg) | 80 (19) | 13 (16) | 12 (23) | 21 (30) | 34 (15) | | |
| Category 4 (SBP ≥140 mm Hg or DBP ≥90 mm Hg) | 47 (11) | 7 (9) | 9 (17) | 15 (21) | 16 (7) | | |
| Body mass index, kg/m ² , mean (SD) | 23.48 (3.25) | 23.14 (3.06) | 23.02 (2.47) | 23.17 (3.58) | 23.79 (3.38) | | |
| Missing values, n (%) | 13 (3) | 0 (0) | 0 (0) | 12 (17) | 1 (0) | | |
| Range, kg/m ² , min-max | 17.96–36.93 | 18.0–34.5 | 17.96–28.85 | 18.1–36.88 | 18.55–36.93 | | |
| Smoking status, n (%) | | | | | | ^a | 1 vs 2, ^a 1 vs 4, ^a 2 vs 3, ^a 2 vs 4, ^a 3 vs 4 ^b |
| Nonsmoker | 273 (65) | 57 (70) | 52 (100) | 40 (57) | 124 (56) | | |
| Occasional smoker | 57 (13) | 16 (20) | 0 (0) | 11 (16) | 30 (14) | | |
| Smoker | 73 (17) | 5 (6) | 0 (0) | 6 (9) | 62 (28) | | |
| Missing values | 20 (5) | 3 (4) | 0 (0) | 13 (19) | 4 (2) | | |
| Fazekas score, n (%) | | | | | | | |
| 0 | 303 (72) | 60 (74) | 15 (29) | 49 (70) | 179 (81) | | |
| 1 | 72 (17) | 14 (17) | 4 (8) | 16 (23) | 38 (17) | | |
| 2 | 0 (0) | 0 (0) | 0 (0) | 0 (0) | 0 (0) | | |
| 3 | 0 (0) | 0 (0) | 0 (0) | 0 (0) | 0 (0) | | |
| Missing values | 48 (11) | 7 (9) | 33 (63) | 5 (7) | 3 (1) | | |
| Total intracranial volume, mL, mean (SD) | 1,450.05 (137.39) | 1,448.41 (138.07) | 1,553.45 (100.05) | 1,424.99 (127.14) | 1,434.19 (137.82) | ^a | 1 vs 2, ^a 2 vs 3, ^a 2 vs 4 ^a |
| Gray matter volume, mL, mean (SD) | 777.41 (88.69) | 829.38 (74.94) | 880.24 (59.62) | 805.25 (64.19) | 725.11 (66.89) | ^a | 1 vs 2, ^a 1 vs 3, ^b 1 vs 4, ^a 2 vs 3, ^a 2 vs 4, ^a 3 vs 4 ^a |
| White matter volume, mL, mean (SD) | 449.79 (55.74) | 430.85 (49.28) | 467.25 (40.38) | 420.51 (46.23) | 461.95 (58.48) | ^a | 1 vs 2, ^a 1 vs 4, ^a 2 vs 3, ^a 3 vs 4 ^a |
| CSF volume, mL, mean (SD) | 222.86 (56.60) | 188.19 (42.88) | 205.97 (36.83) | 199.22 (48.70) | 247.13 (56.18) | ^a | 1 vs 4, ^a 2 vs 4, ^a 3 vs 4 ^a |
| Hippocampal volume, left, mL, mean (SD) | 3.90 (0.45) | 4.17 (0.39) | 4.42 (0.33) | 4.03 (0.35) | 3.65 (0.32) | ^a | 1 vs 2, ^a 1 vs 3, ^b 1 vs 4, ^a 2 vs 3, ^a 2 vs 4, ^a 3 vs 4 ^a |

Continued

Table 2 Characteristics by sample (continued)

| | Total | Sample 1 | Sample 2 | Sample 3 | Sample 4 | p Value | Pairwise comparisons |
|--|-------------|-------------|-------------|-------------|-------------|--------------|--|
| Hippocampal volume, right, mL, mean (SD) | 3.97 (0.43) | 4.20 (0.37) | 4.43 (0.36) | 4.06 (0.36) | 3.74 (0.33) | ^a | 1 vs 2, ^a 1 vs 3, ^a 1 vs 4, ^a 2 vs 3, ^a 2 vs 4, ^a 3 vs 4 ^a |
| Amygdalar volume, left, mL, mean (SD) | 1.68 (0.19) | 1.77 (0.18) | 1.88 (0.14) | 1.71 (0.17) | 1.58 (0.15) | ^a | 1 vs 2, ^a 1 vs 3, ^b 1 vs 4, ^a 2 vs 3, ^a 2 vs 4, ^a 3 vs 4 ^a |
| Amygdalar volume, right, mL, mean (D) | 1.50 (0.16) | 1.58 (0.16) | 1.67 (0.14) | 1.53 (0.14) | 1.43 (0.13) | ^a | 1 vs 2, ^a 1 vs 3, ^b 1 vs 4, ^a 2 vs 3, ^a 2 vs 4, ^a 3 vs 4 ^a |

Abbreviations: BP = blood pressure; DBP = diastolic blood pressure; SBP = systolic blood pressure.

The p Value column specifies significant results of comparisons between samples: empty cells = $p > 0.05$.

The Pairwise comparisons column specifies significant post hoc comparisons between samples: ^a $p < 0.001$, ^b $p < 0.05$, ^c $p < 0.01$.

depicted in figure 1. Inclusion criteria for our study were age between 19 and 40 years, availability of high-resolution structural T1-weighted MRI, and ≥ 1 BP measurements. Participants were excluded in case of previously diagnosed HTN, intake of antihypertensive drugs, or severe diseases (table e-1, doi.org/10.1101/239160).

Standard protocol approvals, registrations, and patient consents

The studies were in agreement with the Declaration of Helsinki and approved by the ethics committee of the medical faculty at the University of Leipzig, Germany (ethics reference numbers: study 1: 154/13-ff; study 2: 385/14-ff; study 3: 097/15-ff; study 4: 263-2009-14122009). Before entering the studies, participants gave written informed consent.

BP measurements

Systolic BP (SBP) and diastolic BP (DBP) were measured at varying times of day using an automatic oscillometric BP monitor (OMRON M500 [samples 1–3], 705IT [sample 4], OMRON Medizintechnik, Mannheim, Germany) after a seated resting period of 5 minutes. In sample 1, 3 measurements were taken from participants' left arms on 3 separate occasions within 2 weeks. In sample 2, 2 measurements were taken from participants' left arms on 2 separate occasions on the same day. In sample 3, BP was measured once before participants underwent MRI. In sample 4, the procedure consisted of 3 consecutive BP measurements, taken from the right arm in intervals of 3 minutes. In each sample, all available measurements per participant were averaged to 1 SBP and 1 DBP value. These averages were used for classification of BP.

Neuroimaging

MRI was performed at the same 3T MAGNETOM Verio Scanner (Siemens, Erlangen, Germany) for all studies with a 32-channel head coil. Whole-brain 3D T1-weighted volumes with a resolution of 1 mm isotropic were acquired for the assessment of brain structure. T1-weighted images in sample 4 were acquired with a standard magnetization-prepared rapid gradient echo protocol (inversion time [TI] 900 ms, repetition time [TR] 2,300 ms, echo time [TE] 2.98 ms, flip angle

[FA] 9°, field of view [FOV] $256 \times 240 \times 176 \text{ mm}^3$, voxel size $1 \times 1 \times 1 \text{ mm}^3$), while T1-weighted images in samples 1–3 resulted from an MP2RAGE protocol (TI1 700 ms, TI2 2,500 ms, TR 5,000 ms, TE 2.92 ms, FA1 4°, FA2 5°, FOV $256 \times 240 \times 176 \text{ mm}^3$, voxel size $1 \times 1 \times 1 \text{ mm}^3$). GM and WM contrast are comparable for the 2 sequence protocols,^{1,2} but additional preprocessing steps were performed for MP2RAGE T1-weighted images (e-Methods, doi.org/10.1101/239160). Fluid-attenuated inversion recovery (FLAIR) images were acquired in all samples for radiologic examination for incidental findings and for Fazekas scale ratings for WM hyperintensities (WMH) (tables 1 and 2).

Data processing and statistical analysis

Details on all analysis methods can be found in the e-Methods (doi.org/10.1101/239160).

BP classification

For statistical analyses, all available BP measurements per participant were averaged to 1 mean SBP and DBP, respectively. Based on these averages, we categorized BP according to the European guidelines for the management of arterial hypertension²³: category 1 (SBP $< 120 \text{ mm Hg}$ and DBP $< 80 \text{ mm Hg}$), category 2 (SBP $120\text{--}129 \text{ mm Hg}$ or DBP $80\text{--}84 \text{ mm Hg}$), category 3 (SBP $130\text{--}139 \text{ mm Hg}$ or DBP $85\text{--}89 \text{ mm Hg}$), and category 4 (SBP $\geq 140 \text{ mm Hg}$ or DBP $\geq 90 \text{ mm Hg}$).

VBM: Association of regional GMV and BP within each sample

For each of the 4 samples, 3T high-resolution T1-weighted 3D whole-brain images were processed using VBM and the diffeomorphic anatomical registration using the exponentiated lie algebra (DARTEL) method^{19,20} within SPM12. Voxel-wise general linear models were performed to relate BP and GMV within each sample: we tested for a continuous relationship between GMV and SBP or DBP, in separate models, with a multiple linear regression t contrast. The overall effect of BP category on GMV was tested with an analysis of variance (ANOVA) F contrast. To assess differences in GMV between BP categories, the following pairwise t comparisons were tested: (1) category 4 vs category 1, (2) category 3 vs category 1, (3) category 2 vs category 1. All

analyses included total intracranial volume (TIV), sex, and age as covariates. The influence of body mass index (BMI) did not significantly contribute to the models and was thus not included as covariate in the analyses. We considered a sample eligible for image-based meta-analysis if its F contrast effects exceeded an uncorrected peak-level threshold of $p < 0.001$. Effects within each sample were explored at cluster-level $p < 0.05$ with family-wise error (FWE) correction for multiple comparisons.

IBMA: Association of regional GMV and BP across samples

To evaluate cumulative results from all samples while considering their heterogeneities, we combined the VBM outcome of each sample in IBMA. Meta-analyses were performed on the unthresholded t maps with seed-based d mapping (SDM) software using default parameters.²⁴ Statistical significance of mean effect size maps was evaluated according to validated thresholds of high meta-analytic sensitivity and specificity²⁴: voxel threshold = $p < 0.005$, peak height threshold = $\text{SDM-Z} > 1.0$, and cluster extent threshold = $k \geq 10$ voxels.

Exploratory IBMA for positive associations were performed in analogy to negative associations as described above.

IBMA of regions of interest (ROI): Association of regional GMV and BP across samples in hippocampus and amygdala

We performed IBMA within atlas-defined masks to test if regional bilateral hippocampal and amygdalar volumes related

to SBP, DBP, and BP categories, respectively. The statistical thresholds were defined as $p < 0.05$, $\text{SDM-Z} > 1.0$, and $k \geq 1$ voxel.

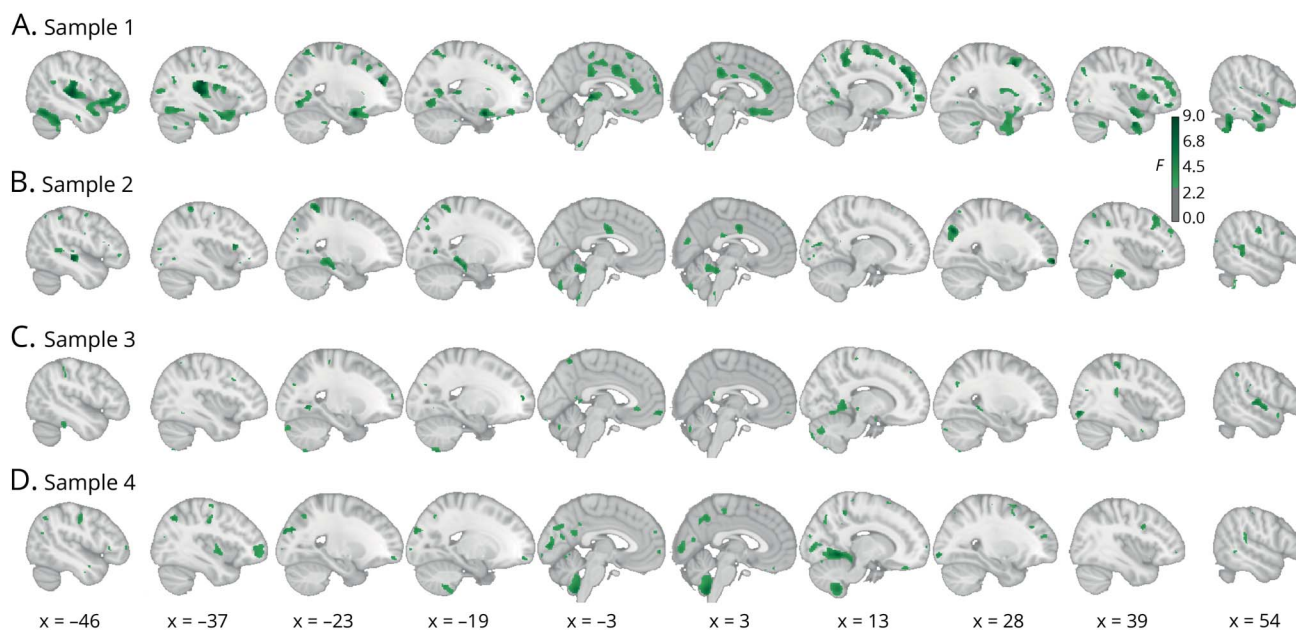
Volumetry: Association of total brain volumes and BP within the pooled sample

In addition to VBM and IBMA, we explored if total brain volumes (average volume over all voxels within a region) differed between BP categories. Specifically, we tested if estimated TIV, total GM volume, total WM volume (WMV), total amount of WMH, total CSF volume (CSFV), total left and right hippocampal, and amygdalar volume differed between BP categories. WMH was assessed by Fazekas scale ratings from FLAIR images.²⁵ For these comparisons within the total sample, we defined correlation models (for SBP and DBP as independent variable, respectively) and ANOVA models for BP category as independent variable. The models included the respective volume as dependent variable, as well as TIV (where applicable), sex, age, and sample (where applicable) as covariates. We considered p values < 0.05 as significant. The analyses were performed with R (3.2.3, R Core Team, 2015, Vienna, Austria; R-project.org/).

Data sharing

Results (i.e., unthresholded whole-brain statistical maps) from VBM analyses of each sample and from all IBMAs can be found online in the public repository NeuroVault for detailed, interactive inspection (neurovault.org/collections/FDWHFSYZ/). Raw data of samples 1–3 are available from openfmri.org/dataset/ds000221/.

Figure 2 Associations between gray matter (GM) volume and blood pressure (BP) within each sample



Sagittal views of voxel-based morphometry F contrast results show the overall effect of BP category on GM volume per sample. Each sample is represented in 1 row (A–D). Slice order runs from left hemisphere (left-hand side of the plot) to right hemisphere (right-hand side of the plot). Color bars represent F values (uncorrected). Sample sizes: sample 1, $n = 81$; sample 2, $n = 52$; sample 3, $n = 70$; sample 4, $n = 220$. 3D volumetric results of these analyses can be inspected in detail on neurovault.org/collections/FDWHFSYZ/.

Results

Sample characteristics

The characteristics of the total sample by BP category are reported in table 1. The total sample included 423 participants between 19 and 40 years of age, of whom 177 were women (42%). Mean (SD) age was 27.7 (5.3) years. SBP, DBP, and BMI differed between BP categories (all $p < 0.001$). An effect of sex yielded that men were more frequent in higher BP categories (all $p < 0.001$).

Table 2 shows differences in characteristics among the 4 included samples. The samples differed in almost all characteristic variables, specifically regarding sex, age, SBP, DBP, smoking status, and brain volumes (all $p < 0.001$).

VBM: Association of regional GMV and BP within each sample

Figure 2 shows differences in regional GMV between BP categories for each of the 4 samples tested with an ANOVA F contrast. Results show significant clusters of various extents that were distributed heterogeneously between the samples. Exploration of sample-specific effects showed a cluster in the left posterior insula for the F contrast (peak Montreal Neurological Institute coordinates $[-38, -24, 24]$, $F = 11.35$, cluster size $k = 1,239$) as well as clusters in left inferior frontal gyrus ($[-42, 34, 0]$, $T = 4.99$, $k = 2,039$) and in right anterior cingulate cortex ($[14, 34, 14]$, $T = 4.44$, $k = 2,086$) for the contrast BP category 4 < 1 in sample 1. In sample 2, the contrast BP category 4 < 1 yielded a cluster in left planum polare ($[-44, -22, -3]$, $T = 10.70$, $k = 1,151$) and the contrast BP category 2 < 1 yielded a trend for a cluster in left middle temporal gyrus ($p_{\text{FWE}} = 0.059$, $[-54, -28, -9]$, $T = 5.41$, $k = 683$). Furthermore, higher DBP was associated with a cluster of lower GMV in left middle temporal gyrus in sample 2 ($[-57, -45, 6]$, $T = 6.03$, $k = 1,180$). All other comparisons yielded no suprathreshold voxels (all $p_{\text{FWE}} > 0.05$). The statistical maps for sample-specific effects can be inspected on NeuroVault.

IBMA: Association of regional GMV and BP across samples

Meta-analytic parametric relations between lower GMV and higher BP

As expected, increases in systolic and diastolic BP were associated with lower GMV. Specifically, higher SBP related to lower GMV in right paracentral/cingulate areas ($[8, -30, 56]$, $\text{SDM-Z} = -3.859$, $k = 288$), bilateral inferior frontal gyrus (IFG, left: $[-40, 30, 0]$, $\text{SDM-Z} = -3.590$, $k = 49$; right: $[-40, 30, 0]$, $\text{SDM-Z} = -3.394$, $k = 16$), bilateral sensorimotor cortex (left: $[-58, -20, 24]$, $\text{SDM-Z} = -3.290$, $k = 146$; right: $[48, 0, 48]$, $\text{SDM-Z} = -3.196$, $k = 127$), bilateral superior temporal gyrus (left: $[-52, -10, 6]$, $\text{SDM-Z} = -3.268$, $k = 78$; right: $[64, -42, 12]$, $\text{SDM-Z} = -3.192$, $k = 42$), bilateral cuneus cortex (left: $[-8, -76, 18]$, $\text{SDM-Z} = -3.019$, $k = 27$; right: $[10, -68, 26]$, $\text{SDM-Z} = -2.937$, $k = 18$), and right thalamus ($[8, -28, 2]$, $\text{SDM-Z} = -2.977$, $k = 45$; figure 3A and table 3). Increases in DBP were related to lower GMV in bilateral

anterior insula (left: $[-36, 26, 6]$, $\text{SDM-Z} = -3.876$, $k = 266$; right: $[34, 10, 8]$, $\text{SDM-Z} = -3.139$, $k = 100$), frontal regions ($[-26, 24, 54]$, $\text{SDM-Z} = -3.820$, $k = 62$), right midcingulate cortex ($[4, -34, 50]$, $\text{SDM-Z} = -3.545$, $k = 246$), bilateral inferior parietal areas (left: $[-46, -26, 48]$, $\text{SDM-Z} = -3.239$, $k = 59$; right: $[44, -44, 50]$, $\text{SDM-Z} = -3.188$, $k = 18$), and right superior temporal gyrus ($[60, 2, -12]$, $\text{SDM-Z} = -2.991$, $k = 35$; figure 3B and table 3).

Meta-analytic differences in regional GMV between BP categories

Meta-analytic results for category 4 (highest BP) compared to category 1 (lowest BP) yielded lower regional GMV in frontal, cerebellar, parietal, occipital, and cingulate regions (figure 3C). Table 3 describes the specific regions with lower GMV, including bilateral IFG (left: $[-52, -28, 12]$, $\text{SDM-Z} = -3.473$, $k = 107$; right: $[40, 30, 26]$, $\text{SDM-Z} = -3.093$, $k = 10$), right midcingulate cortex ($[12, -42, 48]$, $\text{SDM-Z} = -2.854$, $k = 11$), and right precuneus ($[10, -52, 18]$, $\text{SDM-Z} = -2.836$, $k = 21$).

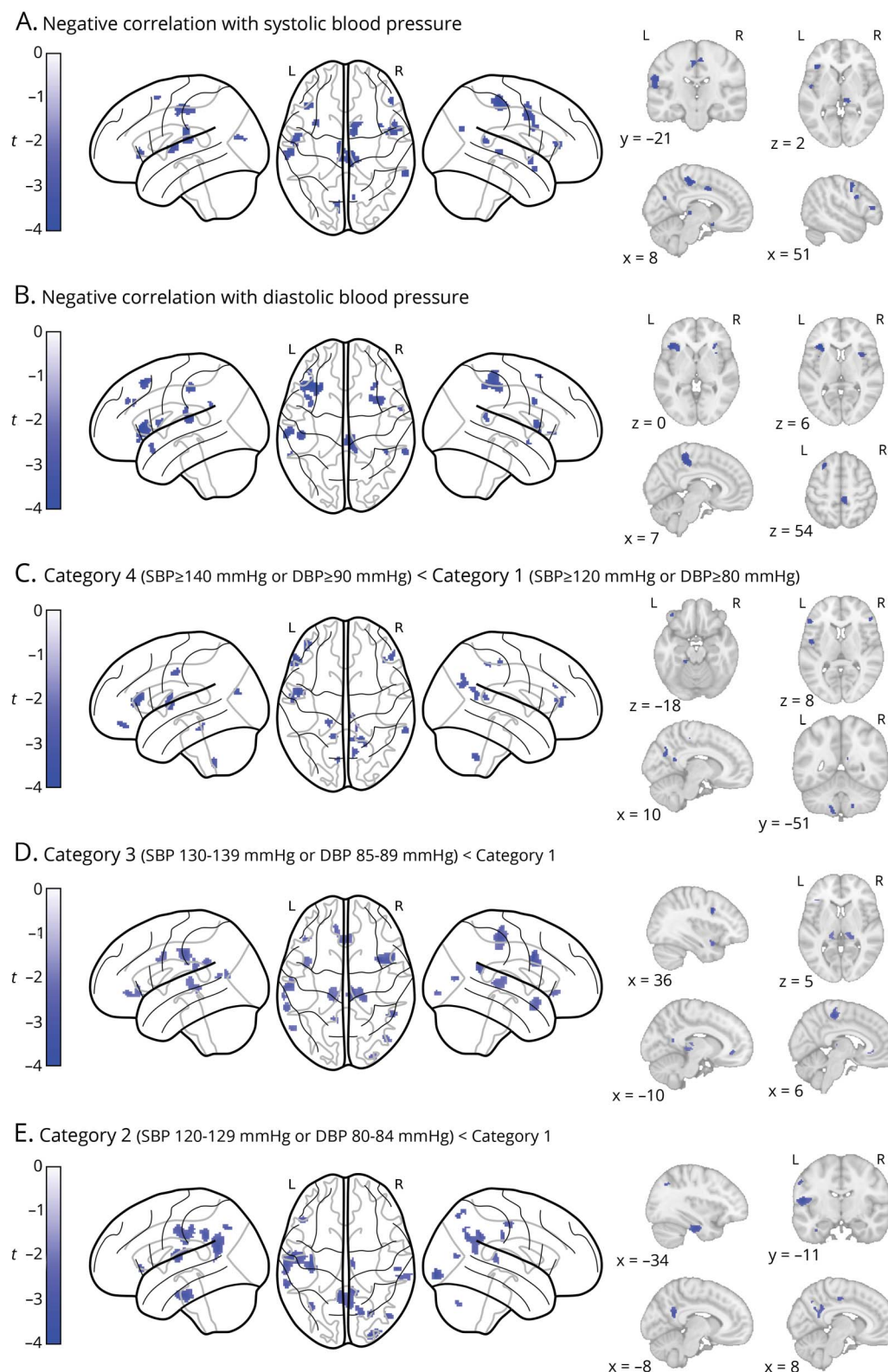
We also compared GMV of individuals at subhypertensive levels (category 3 and 2, respectively) to GMV of individuals in category 1. Figure 3D shows meta-analysis results for the comparison between category 3 and category 1. Compared to category 1, category 3 was associated with lower GMV in bilateral IFG (left: $[-40, 30, 2]$, $\text{SDM-Z} = -2.598$, $k = 24$; right: $[36, 6, 34]$, $\text{SDM-Z} = -3.474$, $k = 179$), sensorimotor cortices (left: $[-60, -20, 36]$, $\text{SDM-Z} = -2.857$, $k = 205$; right: $[6, -28, 54]$, $\text{SDM-Z} = -3.119$, $k = 179$), bilateral middle temporal gyrus (left: $[-56, -64, 16]$, $\text{SDM-Z} = -2.222$, $k = 28$; right: $[48, -50, 20]$, $\text{SDM-Z} = -3.119$, $k = 179$), right insula ($[36, 8, -18]$, $\text{SDM-Z} = -2.523$, $k = 123$), right occipital regions ($[42, -74, 12]$, $\text{SDM-Z} = -2.454$, $k = 25$), left parietal ($[-60, -20, 36]$, $\text{SDM-Z} = -2.857$, $k = 205$), bilateral thalamus (left: $[-12, -32, 0]$, $\text{SDM-Z} = -2.264$, $k = 133$; right: $[20, -32, 6]$, $\text{SDM-Z} = -2.384$, $k = 133$), left anterior cingulate cortex ($[-10, 36, -6]$, $\text{SDM-Z} = -2.384$, $k = 102$), and left precuneus ($[-12, -54, 14]$, $\text{SDM-Z} = -2.187$, $k = 20$; table 3).

Figure 3E illustrates brain regions that yielded lower meta-analytic GMV comparing category 2 to category 1. These include left frontal regions ($[-54, -10, 14]$, $\text{SDM-Z} = -3.407$, $k = 230$), right inferior occipital gyrus ($[30, -96, -8]$, $\text{SDM-Z} = -3.290$, $k = 102$), bilateral temporal regions (left: $[-34, -16, -30]$, $\text{SDM-Z} = -3.164$, $k = 133$; right: $[46, -74, 12]$, $\text{SDM-Z} = -2.734$, $k = 26$), left precuneus ($[-8, -54, 22]$, $\text{SDM-Z} = -3.084$, $k = 433$), and inferior parietal regions (supramarginal, $[54, -24, 32]$, $\text{SDM-Z} = -2.968$, $k = 31$, and angular gyri, $[-36, -64, 42]$, $\text{SDM-Z} = -2.827$, $k = 30$), as well as midcingulate cortex ($[8, -18, 46]$, $\text{SDM-Z} = -2.647$, $k = 32$; table 3).

Meta-analytic differences in regional hippocampal and amygdalar volumes between BP categories

In this IBMA ROI comparison, higher SBP was correlated with lower bilateral posterior medial hippocampal volume (figure 4). Higher DBP was correlated with lower left hippocampal volume and lower right anterior hippocampal

Figure 3 Meta-analytic differences in gray matter (GM) volume between blood pressure (BP) categories



Glass brain views of image-based meta-analysis results for the BP category contrasts of interest with relevant slice views below (A–E). A and B depict associations between higher systolic BP (SBP)/diastolic BP (DBP), respectively, and lower GM volume, i.e., negative correlations. Blue clusters indicate meta-analytic GM volume differences for the given contrast at a voxel threshold of $p < 0.005$ with peak height threshold of seed-based d mapping (SDM) $Z < -1.0$ and cluster extent threshold of $k \geq 10$ (validated for high meta-analytic sensitivity and specificity²⁴). Color bars represent SDM- Z values. 3D volumetric results of these analyses can be inspected in detail on neurovault.org/collections/FDWHFSYZ/. L = left hemisphere; R = right hemisphere.

Table 3 Image-based meta-analysis results of regional gray matter (GM) volume differences associated with blood pressure (BP)

| | MNI, x,y,z | SDM-Z | <i>P</i> Value | <i>k</i> | Peak description | <i>Q</i> | <i>I</i> ² |
|--------------------------------------|------------|--------|-------------------|----------|---|----------|-----------------------|
| Negative correlation with SBP | 8,-30,56 | -3.859 | 0.000 | 288 | Right paracentral lobule | 0.000 | 0.0 |
| | -40,30,0 | -3.590 | 0.000 | 49 | Left inferior frontal gyrus (p. triangularis) | 0.053 | 0.0 |
| | 36,6,34 | -3.394 | 0.000 | 16 | Right inferior frontal gyrus (pars opercularis) | 0.000 | 0.0 |
| | 10,2,40 | -3.325 | 0.001 | 45 | Right midcingulate cortex | 0.000 | 0.0 |
| | -58,-20,24 | -3.290 | 0.001 | 146 | Left postcentral gyrus | 0.000 | 0.0 |
| | -52,-10,6 | -3.268 | 0.001 | 78 | Left superior temporal gyrus | 0.000 | 0.0 |
| | 48,32,10 | -3.204 | 0.001 | 27 | Right inferior frontal gyrus (p. triangularis) | 0.000 | 0.0 |
| | 48,0,48 | -3.196 | 0.001 | 127 | Right precentral gyrus | 0.000 | 0.0 |
| | 64,-42,12 | -3.192 | 0.001 | 42 | Right superior temporal gyrus | 0.000 | 0.0 |
| | 6,8,-18 | -3.110 | 0.001 | 40 | Right subgenual cingulate cortex | 0.000 | 0.0 |
| | 50,8,28 | -3.045 | 0.002 | 26 | Right inferior frontal gyrus (pars opercularis) | 0.000 | 0.0 |
| | -8,-76,18 | -3.019 | 0.002 | 27 | Left cuneus cortex | 0.175 | 0.0 |
| | 8,-28,2 | -2.977 | 0.002 | 45 | Right thalamus | 0.000 | 0.0 |
| | 10,-68,26 | -2.937 | 0.002 | 18 | Right cuneus cortex | 0.000 | 0.0 |
| | 58,4,-8 | -2.934 | 0.002 | 32 | Right temporal pole | 0.000 | 0.0 |
| | -28,10,60 | -2.896 | 0.003 | 19 | Left middle frontal gyrus | 0.000 | 0.0 |
| | -52,-12,42 | -2.860 | 0.003 | 10 | Left postcentral gyrus | 0.116 | 0.0 |
| Negative correlation with DBP | -36,26,6 | -3.876 | 0.000 | 266 | Left insula | 0.000 | 0.0 |
| | -26,24,54 | -3.820 | 0.000 | 62 | Left middle frontal gyrus | 0.000 | 0.0 |
| | 4,-34,50 | -3.545 | 0.000 | 246 | Right midcingulate cortex | 0.000 | 0.0 |
| | -60,-24,14 | -3.462 | 0.000 | 90 | Left supramarginal gyrus | 0.000 | 0.0 |
| | -46,-26,48 | -3.239 | 0.001 | 59 | Left inferior parietal lobule | 0.000 | 0.0 |
| | 44,-44,50 | -3.188 | 0.001 | 18 | Right inferior parietal lobule | 0.257 | 0.0 |
| | 36,8,32 | -3.180 | 0.001 | 25 | Right inferior frontal gyrus (pars opercularis) | 0.000 | 0.0 |
| | 34,10,8 | -3.139 | 0.001 | 100 | Right insula | 0.000 | 0.0 |
| | 28,14,60 | -3.069 | 0.001 | 12 | Right superior frontal gyrus | 0.000 | 0.0 |
| | 62,-44,16 | -2.991 | 0.002 | 35 | Right superior temporal gyrus | 0.000 | 0.0 |
| | -38,14,-20 | -2.983 | 0.002 | 30 | Left temporal pole | 0.000 | 0.0 |
| | 60,2,-12 | -2.862 | 0.003 | 13 | Right superior temporal gyrus | 0.189 | 0.0 |
| | -38,40,32 | -2.845 | 0.003 | 14 | Left middle frontal gyrus | 0.000 | 0.0 |
| | 30,28,0 | -2.796 | 0.003 | 14 | Right insula | 0.000 | 0.0 |
| | -36,8,10 | -2.788 | 0.003 | 24 | Left insula | 0.000 | 0.0 |
| | -58,-46,30 | -2.750 | 0.004 | 11 | Left supramarginal gyrus | 0.000 | 0.0 |
| | -34,32,32 | -2.734 | 0.004 | 11 | Left middle frontal gyrus | 0.201 | 0.0 |

Continued

Table 3 Image-based meta-analysis results of regional gray matter (GM) volume differences associated with blood pressure (BP) (continued)

| | MNI, x,y,z | SDM-Z | P Value | k | Peak description | Q | I ² |
|--|-------------|--------|---------|-----|--|-------|----------------|
| Category 4 (SBP ≥140 mm Hg or DBP ≥90 mm Hg) < category 1 (SBP <120 mm Hg and DBP <80 mm Hg) | -52,28,12 | -3.473 | 0.000 | 107 | Left inferior frontal gyrus (pars triangularis) | 0.324 | 3.9 |
| | -48,-4,4 | -3.322 | 0.000 | 93 | Left rolandic operculum | 0.297 | 1.8 |
| | 18,-52,-48 | -3.097 | 0.001 | 40 | Right cerebellum, hemispheric lobule VIIIb | 0.000 | 0.0 |
| | 40,30,26 | -3.093 | 0.001 | 10 | Right inferior frontal gyrus (pars triangularis) | 0.000 | 0.0 |
| | 48,32,10 | -3.064 | 0.001 | 48 | Right inferior frontal gyrus (pars triangularis) | 0.000 | 0.0 |
| | -38,48,-16 | -3.014 | 0.001 | 40 | Left inferior frontal gyrus (pars orbitalis) | 0.000 | 0.0 |
| | -54,-12,42 | -2.940 | 0.002 | 30 | Left postcentral gyrus | 0.000 | 0.0 |
| | -8,-76,18 | -2.936 | 0.002 | 14 | Left cuneus | 0.000 | 0.0 |
| | -16,-36,-18 | -2.872 | 0.002 | 24 | Left cerebellum, hemispheric lobule V | 0.000 | 0.0 |
| | 12,-42,48 | -2.854 | 0.002 | 11 | Right midcingulate cortex | 0.000 | 0.0 |
| | -12,-50,-56 | -2.849 | 0.002 | 30 | Left cerebellum, hemispheric lobule IX | 0.325 | 4.0 |
| | 10,-52,18 | -2.836 | 0.002 | 21 | Right precuneus | 0.000 | 0.0 |
| | 64,-44,14 | -2.824 | 0.002 | 26 | Right superior temporal gyrus | 0.000 | 0.0 |
| | 10,-66,28 | -2.821 | 0.002 | 56 | Right precuneus | 0.000 | 0.0 |
| | 6,-28,50 | -2.792 | 0.003 | 16 | Right midcingulate cortex | 0.025 | 0.0 |
| | 18,-54,22 | -2.765 | 0.003 | 15 | Right precuneus | 0.000 | 0.0 |
| Category 3 (SBP 130–139 mm Hg or DBP 85–89 mm Hg) < category 1 | 36,6,34 | -3.474 | 0.000 | 179 | Right inferior frontal gyrus (pars opercularis) | 0.000 | 0.0 |
| | 6,-28,54 | -3.119 | 0.000 | 179 | Right posterior-medial frontal gyrus | 0.127 | 0.0 |
| | 48,-50,20 | -2.917 | 0.000 | 74 | Right middle temporal gyrus | 0.000 | 0.0 |
| | -60,-20,36 | -2.857 | 0.000 | 205 | Left postcentral gyrus | 0.000 | 0.0 |
| | -40,30,2 | -2.598 | 0.000 | 24 | Left inferior frontal gyrus (pars triangularis) | 0.000 | 0.0 |
| | 36,8,-18 | -2.523 | 0.001 | 123 | NA (Right insula) | 0.000 | 0.0 |
| | 42,-74,12 | -2.454 | 0.001 | 25 | Right middle occipital gyrus | 0.200 | 0.0 |
| | -62,-42,28 | -2.433 | 0.001 | 41 | Left supramarginal gyrus | 0.000 | 0.0 |
| | 20,-32,6 | -2.384 | 0.001 | 133 | Right thalamus | 0.000 | 0.0 |
| | -10,36,-6 | -2.384 | 0.001 | 102 | Left anterior cingulate cortex | 0.000 | 0.0 |
| | 28,-94,-4 | -2.373 | 0.001 | 14 | Right inferior occipital gyrus | 0.000 | 0.0 |
| | -12,-32,0 | -2.264 | 0.002 | 133 | Left thalamus | 0.237 | 0.0 |
| | -56,-64,16 | -2.222 | 0.002 | 28 | Left middle temporal gyrus | 0.050 | 0.0 |
| | -40,8,30 | -2.197 | 0.002 | 82 | Left precentral gyrus | 0.000 | 0.0 |
| | -12,-54,14 | -2.187 | 0.002 | 20 | Left precuneus | 0.000 | 0.0 |
| Category 2 (SBP 120–129 mm Hg or DBP 80–84 mm Hg) < category 1 | -54,-10,14 | -3.407 | 0.000 | 230 | Left rolandic operculum | 0.016 | 0.0 |
| | 30,-96,-8 | -3.290 | 0.000 | 102 | Right inferior occipital gyrus | 0.038 | 0.0 |

Continued

Table 3 Image-based meta-analysis results of regional gray matter (GM) volume differences associated with blood pressure (BP) (continued)

| MNI, x,y,z | SDM-Z | <i>p</i> Value | <i>k</i> | Peak description | <i>Q</i> | <i>I</i> ² |
|-------------|--------|----------------|----------|---|----------|-----------------------|
| -34,-16,-30 | -3.164 | 0.000 | 133 | Left fusiform gyrus | 0.000 | 0.0 |
| -8,-54,22 | -3.084 | 0.000 | 433 | Left precuneus | 0.000 | 0.0 |
| 54,-24,32 | -2.968 | 0.000 | 31 | Right supramarginal gyrus | 0.019 | 0.0 |
| -46,28,0 | -2.942 | 0.000 | 41 | Left inferior frontal gyrus (p. triangularis) | 0.000 | 0.0 |
| -64,-20,30 | -2.939 | 0.000 | 227 | Left postcentral gyrus | 0.000 | 0.0 |
| -62,-42,34 | -2.876 | 0.000 | 68 | Left supramarginal gyrus | 0.000 | 0.0 |
| -36,-64,42 | -2.827 | 0.001 | 30 | Left angular gyrus | 0.000 | 0.0 |
| 18,-72,54 | -2.804 | 0.001 | 40 | Right superior parietal lobule | 0.083 | 0.0 |
| 46,-74,12 | -2.734 | 0.001 | 26 | Right middle temporal gyrus | 0.000 | 0.0 |
| 8,-18,46 | -2.647 | 0.001 | 32 | Right midcingulate cortex | 0.000 | 0.0 |
| 56,-32,12 | -2.470 | 0.002 | 52 | Right superior temporal gyrus | 0.000 | 0.0 |
| 28,-72,-38 | -2.413 | 0.002 | 23 | Right cerebellum, crus I | 0.000 | 0.0 |
| -62,-22,-30 | -2.403 | 0.003 | 11 | NA (Left inferior temporal gyrus) | 0.000 | 0.0 |

Abbreviations: DBP = diastolic blood pressure; MNI = Montreal Neurologic Institute; SBP = systolic blood pressure; SDM = seed-based *d* mapping. Image-based meta-analysis results of significant clusters yielding lower GM volume for the respective contrast of interest. Columns indicate cluster-specific MNI coordinates of peak voxels, meta-analytic SDM-Z-value, meta-analytic *p* value, number of voxels in cluster, and anatomical label of the peak voxel. Anatomical labels were assigned using SPM's Anatomy toolbox. *Q* and *I*² are measures of meta-analytic heterogeneity. Voxel threshold was set to *p* < 0.005, peak height threshold was set to SDM-Z > 1.0, and cluster extent threshold was set to *k* ≥ 10 voxels as recommended in reference 24. Final voxel size was 2 × 2 × 2 mm³.

volume. Furthermore, all higher BP categories were associated with lower regional hippocampal volume when compared to the lowest BP category 1 (figure 4). Compared to category 1, BP category 4 was predominantly associated with lower left medial posterior hippocampus volume and category 3 with lower bilateral posterior and left medial hippocampus volume across samples. Lower volume comparing categories 2 and 1 was predominantly located in left lateral anterior hippocampus. Category 4 vs category 1 and the associations with higher SBP and DBP also yielded significantly lower regional volume in bilateral amygdala, respectively. Effect sizes highly varied across samples (figure 4).

Meta-analytic relations between higher GMV and higher BP

Exploratory analyses also revealed associations between higher BP and higher GMV (figure e-1, table e-2, doi.org/10.1101/239160, and NeuroVault maps). However, the cumulative positive effects are comparably weaker than the cumulative negative results (table 3, negative: 17 out of 34 clusters from parametric analyses with SDM-Z > 3.0; positive: 0 out of 28 clusters from parametric analyses with SDM-Z > 3.0), they show greater heterogeneity across studies (negative: maximum *I*² = 4.0; positive: maximum *I*² = 56.3), and they seem to appear primarily in regions where standard preprocessing of brain tissue is suboptimal (e.g., in cerebellum/inferior occipital regions²⁶). We therefore regard these findings as questionable overall. By also providing the results as statistical

maps on NeuroVault, future investigations can use the data for reliability analyses of potential positive associations.

Volumetry in pooled sample: Association of total brain volumes and BP

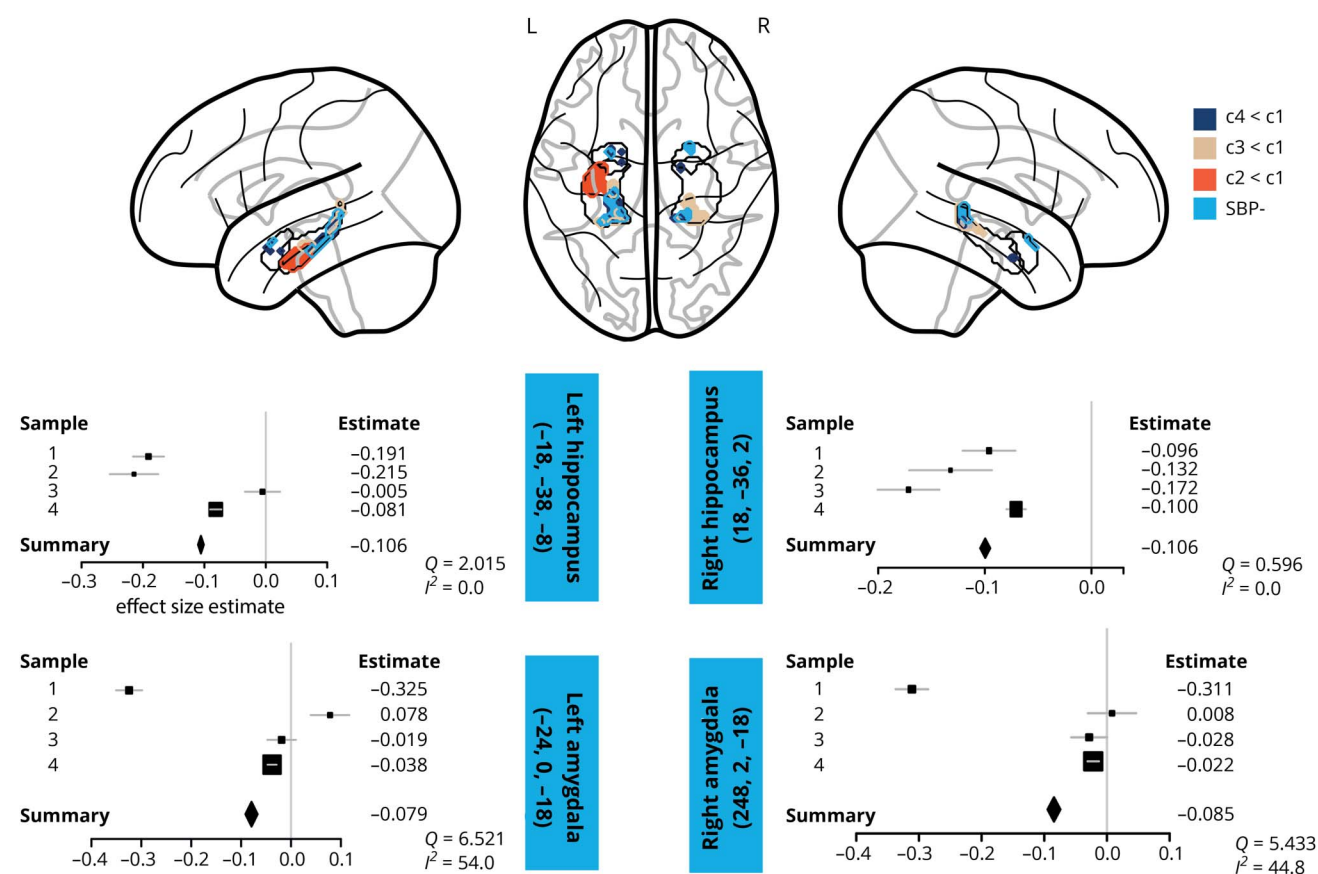
All associations of volumetric brain measures (TIV, total GMV, total WMV, total CSFV, total hippocampal, total amygdalar volume, and total WMH) with SBP or DBP in the correlation models, or with BP categories in the ANOVA models, were below the statistical threshold (all *p* > 0.05, table 1).

Discussion

In this image-based meta-analysis of 4 previously unpublished independent samples, we found that elevated, subhypertensive BP was correlated with lower GMV in several brain regions, including parietal, frontal, and subcortical structures in young adults (<40 years). These regions are consistent with the lower regional GMV observed in middle-aged and older individuals with HTN.^{5,6,9-11,15} Our results show that BP-associated GM alterations emerge earlier in adulthood than previously assumed and continuously across the range of BP.

Interestingly, we found that BP was associated with lower hippocampal volume. In older individuals, the hippocampal formation and surrounding structures are known to be affected by HTN.^{5,8-10,15} In a meta-analytic evaluation of HTN

Figure 4 Meta-analytic differences in volumes of hippocampus and amygdala (region of interest [ROI] analysis)



Upper part of plot: Glass brain views of image-based meta-analysis ROI results for the BP category contrasts of interest in bilateral hippocampus and amygdala masks. Voxel threshold was set to $p < 0.05$ with a peak height threshold of seed-based d mapping (SDM) $Z < -1.0$ and a cluster extent threshold of $k \geq 1$. Lower part of plot: Exemplary forest plots of sample-specific peak voxels' effect sizes for the negative correlation with systolic BP (SBP) in the respective ROI. The box sizes are determined by each sample's weight. Light blue boxes include ROI name and Montreal Neurologic Institute coordinates of the peak voxel. Q and I^2 are measures of meta-analytic heterogeneity. Definition of BP categories: category 1 (SBP < 120 mm Hg and diastolic BP [DBP] < 80 mm Hg), category 2 (SBP 120–129 mm Hg or DBP 80–84 mm Hg), category 3 (SBP 130–139 mm Hg or DBP 85–89 mm Hg), and category 4 (SBP ≥ 140 mm Hg or DBP ≥ 90 mm Hg). L = left hemisphere; R = right hemisphere; SBP- = negative correlation with SBP.

effects on total GMV and on hippocampal volume, lower volumes across studies were only consistently found for the hippocampus.¹⁵ In analogy to those findings, our results showed that hippocampal volume was affected by higher BP in a considerably younger sample. It should be mentioned that the effects in hippocampus only exceeded statistical thresholds in ROI analyses, similar to previous reports of lower hippocampal volume in older samples with manifest HTN that were all ROI-based.^{5,9,10,15} As potential pathophysiologic explanations, it has been proposed that medial temporal (and frontal regions) might be especially sensitive to effects of pulsation, hypoperfusion, and ischemia, which often result from increasing pressure.^{3,15}

We furthermore observed correlations between lower amygdalar and thalamic volumes and higher BP, notably already below levels that are currently regarded as hypertensive. Amygdalar and thalamic nuclei are substantially involved in BP regulation as they receive baroreceptor afferent signals via the brainstem and mesencephalic nuclei, relaying these signals

to primary cortical regions of viscerosensory integration, such as anterior cingulate cortex and insula.²⁷ It has been shown that lower amygdalar volume correlates with increased BP reactivity during cognitive demand among young normotensive adults.¹⁸ Previous studies have reported lower thalamic volume in HTN,⁵ heart failure,²⁸ asymptomatic carotid stenosis,²⁹ and aging.³⁰ Higher systolic BP has also been related to higher mean diffusivity of WM thalamic radiations.¹³ Our results are in line with accumulating evidence of amygdalar and thalamic involvement in cardiovascular (dys-) regulation but may also reflect early pathology in these regions. For example, occurrence of neurofibrillary tangles in thalamus has also been reported in the earliest stages of AD neuropathology.³¹

Beyond subcortical structures, we found lower volumes in cortical regions: cingulate volume and insular volume were markedly lower with higher DBP in the meta-analysis results and in the individual analyses of sample 1. As noted above, these regions constitute primary cortical sites of afferent viscerosensory integration and modulate homeostasis via

efferents to brainstem nuclei.²⁷ Lesions in cingulate cortex and insula result in altered cardiovascular regulation, increased sympathetic tone,^{32,33} and myocardial injury.³⁴ Both regions are also critical for the appraisal and regulation of emotion and stress.²⁷ Thus, structural alterations in these regions may contribute to insidious BP elevations via sympathetic pathways.

Frontal and parietal volumes were affected in all our statistical comparisons. The precuneus cortex, especially, was associated with lower GMV in BP categories 4, 3, and 2 compared to category 1. Our results of lower BP-related GMV in regions such as hippocampal, frontal, and parietal areas highlight specific brain regions that are known to be vulnerable to putative vascular or neurodegenerative damage mechanisms.^{5,6,8–11,15,35} Raised midlife BP is not only known to be a major risk factor for vascular dementia, but some reports suggest a link between HTN and AD-type pathophysiology.^{3,4} For example, in neuropathologic studies, raised midlife BP has been associated with lower post-mortem brain weight, increased numbers of hippocampal neurofibrillary tangles, and higher numbers of hippocampal and cortical neuritic plaques.⁸ Similarly, a potential pathophysiological link between HTN and AD has been supported by noninvasive MRI studies: regions referred to as AD-signature regions (including inferior parietal, precuneus cortices, and medial temporal structures) have been associated with cortical thinning years before clinical AD symptoms arise³⁵ and with brain volume reductions predicted by increasing BP from middle to older age.⁵ In light of these previous results, our findings of lower BP-related GMV in AD signature regions may be indicative of a link to AD pathology at an even earlier age; however, this cannot be causally inferred from our cross-sectional data. In the study by Power et al.,⁵ BP also predicted volume loss in non-AD-typical brain regions, such as frontal lobe and subcortical GM, which may relate to other (than AD-related) pathophysiological mechanisms. A similar pattern seems to be reflected in our findings of lower GMV related to higher BP in non-AD-typical regions.

Some previous studies did not find relations between HTN and lower brain volumes, but associated HTN with other forms of structural or functional brain alterations, such as WM injury³⁶ or reduced cerebral perfusion.³⁷ A key aspect of diverging results is the heterogeneity of methods used to assess brain volumes. Earlier investigations of BP effects on brain tissues have applied manual or automated volumetric methods to quantify total brain volumes in preselected ROIs.^{9,10,12} The focus of this study was to employ computational anatomy methods to assess regional GM differences across the whole brain. We found significant differences between BP groups using VBM but not in the analysis of total brain volumes. This supports the view that VBM is a sensitive measure to quantify regional morphologic differences³⁸ that might be undetected from the analysis of total brain volumes alone. In addition, we employed random-effects IBMA, which results in effects that are consistent across studies and that may otherwise be

neglected at subthreshold. Investigating effects of BP on regional vs total brain volumes at all stages of health and disease thus warrants further research with standardized methods to identify neuropathologic mechanisms.

Our data, however, do not allow inference on causality between lower brain volumes and HTN, which likely involves complex interactions of different pathophysiological mechanisms that still need to be fully elucidated. It is assumed that vascular stiffness, endothelial failure, and a dysfunctional blood–brain barrier are precursors of cerebral small and large vessel disease that reduce cerebral blood flow, disturb autor-regulatory adjustment, and decrease vasomotor reactivity, which may impair perivascular central nervous waste clearance systems.³ These mechanisms have also been suggested to potentially underlie the epidemiologic connection between vascular risk factors, such as HTN, and AD.³ The similarities between our findings and AD signature regions (see above) would also be consistent with this putative link. Consequently, demyelination, apoptosis, and intoxication of neurons and glial cells, as well as GM and WM necrosis, accumulate and may be reflected in neuroimaging on a macroscopic scale. Lower GMV assessed by VBM, as reported in our study, can thus arise from neuronal loss, but also from alterations of glial cells or composition of microstructural or metabolic tissue properties.³⁹ Our findings point to an early effect of such mechanisms on GM integrity, which is present in the absence of overt disease, such as HTN, and in young age. Indicators of early atherosclerosis in major peripheral arteries can already be detected in youth.⁴⁰ Recently, arterial stiffness has also been associated with WM and GM alterations among adults between 24 and 76 years of age.⁴¹ Thus, early and subtle vascular changes, deficient cerebral perfusion, and impaired perivascular clearance systems may initiate and sustain neuropathology from early to late adulthood.

The cross-sectional design of our 4 study samples limits the interpretation frame for the results presented. Causality between BP and potential brain damage cannot be assessed with these data but is crucial for implications of early signs of cerebrovascular disease. Furthermore, the study samples differed regarding recruitment, sex distribution, sample size, prevalence of high BP, and data acquisition methods (BP and MRI), which might not represent the general population or standard acquisition protocols: similar to German prevalence,⁴² men had higher BP in our study. We thus included sex as covariate in all our analyses to adjust for sex effects. We did not perform separate analyses for men and women given that 1 of the 4 samples included only men. However, the topic of sex differences in brain structure related to BP is an interesting open question for future investigations. In sample 3, only 1 BP measurement was recorded, which could be biased due to white coat hypertension or BP variability. Practice guidelines recommend an average of ≥ 2 seated readings obtained on ≥ 2 occasions to provide a more accurate estimate of an individual's BP level.^{23,43,44} By combining the samples in random-effects IBMA, we considered the limitations of each sample

and accounted for within- and between-sample heterogeneity and evaluated effects cumulatively. Moreover, this approach enabled us to investigate the expected small effects of BP-related GM alterations in a well-powered total sample of over 400 young adults. To further ensure that the results are not substantially influenced by the heterogeneity of BP measurements across studies, we recalculated the parametric SBP analysis (figure 3A) with only the first SBP reading in each study. The results of this additional analysis are strikingly similar to the results reported here (table e-3 and figure e-2, doi.org/10.1101/239160). HTN is also the most important risk factor for WM damage^{3,12} and subclinical WM injury in relation to elevated BP levels has recently been reported in 19- to 63-year-old adults.¹³ As our study included only GM measures, we cannot assess mediating effects of WM injury on GMV differences. We did not observe any significant differences in Fazekas scores for WMH between BP categories, likely due to their lower sensitivity and poorer specificity as a proxy for vascular disease in a subclinical sample of young adults with (mostly) normal BP.

Our study shows that BP-related brain alterations may occur in early adulthood and at BP levels below current thresholds for manifest HTN. Contrary to assumptions that BP-related brain damage arises over years of manifest disease, our data suggest that subtle pressure-related GM alterations can be observed in young adults without previously diagnosed HTN. Considering our results, large-scale cohort studies should investigate whether subhypertensive BP and related brain changes in early adulthood increase the risk for subsequent development of CVD later in life. Gaining insights whether and how the brain is globally affected by vascular changes or if these are specific to susceptible regions could help identify neuroimaging biomarkers for the earliest stages of CVD. Such data would provide evidence for future guidelines to formulate informed recommendations for BP management in young adults, which are critical for the prevention of CVD. Lifestyle interventions and neurobehavioral therapy have recently been suggested to benefit CVD prevention.¹⁷ Our results highlight the importance of taking BP levels as a continuous measure into consideration, which could help initiate such early preventive measures.

Author contributions

Study concept and design: H.L. Schaare, Dr. Villringer. Statistical analysis: H.L. Schaare. Acquisition or interpretation of data: all authors. Drafting of the manuscript: H.L. Schaare, Dr. Villringer. Critical revision of the manuscript: all authors.

Acknowledgment

The authors thank the volunteers for their participation and the researchers, technicians, and students who planned, collected, entered, and curated data used in this article.

Study funding

Max Planck Institute for Human Cognitive and Brain Sciences.

Disclosure

The authors report no disclosures relevant to the manuscript. Go to Neurology.org/N for full disclosures.

Publication history

Received by *Neurology* January 9, 2018. Accepted in final form October 15, 2018.

References

- Forouzanfar MH, Afshin A, Alexander LT, et al. Global, regional, and national comparative risk assessment of 79 behavioural, environmental and occupational, and metabolic risks or clusters of risks, 1990–2015: a systematic analysis for the Global Burden of Disease Study 2015. *Lancet* 2016;388:1659–1724.
- NCD Risk Factor Collaboration (NCD-RisC). Worldwide trends in blood pressure from 1975 to 2015: a pooled analysis of 1479 population-based measurement studies with 19.1 million participants. *Lancet* 2016;389:634–647.
- Iadecola C, Yaffe K, Biller J, et al. Impact of hypertension on cognitive function: a scientific statement from the American Heart Association. *Hypertension* 2016;68:e67–e94.
- Norton S, Matthews FE, Barnes DE, Yaffe K, Brayne C. Potential for primary prevention of Alzheimer's disease: an analysis of population-based data. *Lancet Neurol* 2014;13:788–794.
- Power MC, Schneider AL, Wruck L, et al. Life-course blood pressure in relation to brain volumes. *Alzheimers Dement* 2016;12:890–899.
- Hajjar J, Zhao P, Alsop D, et al. Association of blood pressure elevation and nocturnal dipping with brain atrophy, perfusion and functional measures in stroke and non-stroke individuals. *Am J Hypertens* 2010;23:17–23.
- Launer LJ, Lewis CE, Schreiner PJ, et al. Vascular factors and multiple measures of early brain health: CARDIA brain MRI study. *PLoS One* 2015;10:e0122138.
- Petrovitch H, White LR, Izmirlian G, et al. Midlife blood pressure and neuritic plaques, neurofibrillary tangles, and brain weight at death: the HAAS. *Neurobiol Aging* 2000;21:57–62.
- den Heijer T, Launer LJ, Prins ND, et al. Association between blood pressure, white matter lesions, and atrophy of the medial temporal lobe. *Neurology* 2005;64:263–267.
- Raz N, Lindenberg U, Rodrigue KM, et al. Regional brain changes in aging healthy adults: general trends, individual differences and modifiers. *Cereb Cortex* 2005;15:1676–1689.
- Leritz EC, Salat DH, Williams VJ, et al. Thickness of the human cerebral cortex is associated with metrics of cerebrovascular health in a normative sample of community dwelling older adults. *Neuroimage* 2011;54:2659–2671.
- Debetto S, Seshadri S, Beiser A, et al. Midlife vascular risk factor exposure accelerates structural brain aging and cognitive decline. *Neurology* 2011;77:461–468.
- Maillard P, Seshadri S, Beiser A, et al. Effects of systolic blood pressure on white-matter integrity in young adults in the Framingham Heart Study: a cross-sectional study. *Lancet Neurol* 2012;11:1039–1047.
- Muller M, Sigurdsson S, Kjartansson O, et al. Joint effect of mid- and late-life blood pressure on the brain: the AGES-Reykjavik study. *Neurology* 2014;82:2187–2195.
- Beauchet O, Celle S, Roche F, et al. Blood pressure levels and brain volume reduction: a systematic review and meta-analysis. *J Hypertens* 2013;31:1502–1516.
- Olsen MH, Angell SY, Asma S, et al. A call to action and a lifecourse strategy to address the global burden of raised blood pressure on current and future generations: the Lancet Commission on Hypertension. *Lancet* 2016;388:2665–2712.
- Grossman DC, Bibbins-Domingo K, Curry SJ, et al. Behavioral counseling to promote a healthful diet and physical activity for cardiovascular disease prevention in adults without cardiovascular risk factors. *JAMA* 2017;318:167.
- Gianaros PJ, Sheu LK, Matthews KA, Jennings JR, Manuck SB, Hariri AR. Individual differences in stressor-evoked blood pressure reactivity vary with activation, volume, and functional connectivity of the amygdala. *J Neurosci* 2008;28:990–999.
- Ashburner J, Friston KJ. Voxel-based morphometry: the methods. *Neuroimage* 2000;11:805–821.
- Ashburner J. A fast diffeomorphic image registration algorithm. *Neuroimage* 2007;38:95–113.
- Mendes N, Oligschlaeger S, Lauckner ME, et al. A functional connectome phenotyping dataset including cognitive state and personality measures. *bioRxiv* 2017. Available at: <https://www.biorxiv.org/content/early/2017/07/18/164764>. Accessed July 19, 2017.
- Loeffler M, Engel C, Ahnert P, et al. The LIFE-Adult-Study: objectives and design of a population-based cohort study with 10,000 deeply phenotyped adults in Germany. *BMC Public Health* 2015;15:691.
- Mancia G, Fagard R, Narkiewicz K, et al. 2013 ESH/ESC Guidelines for the management of arterial hypertension. *Eur Heart J* 2013;34:2159–2219.
- Radua J, Mataix-Cols D, Phillips ML, et al. A new meta-analytic method for neuroimaging studies that combines reported peak coordinates and statistical parametric maps. *Eur Psychiatry* 2012;27:605–611.
- Fazekas F, Chawluk J, Alavi A, Hurtig H, Zimmerman R. MR signal abnormalities at 1.5 T in Alzheimer's dementia and normal aging. *Am J Roentgenol* 1987;149:351–356.
- Diedrichsen J. A spatially unbiased atlas template of the human cerebellum. *Neuroimage* 2006;33:127–138.
- Critchley HD, Harrison NA. Visceral influences on brain and behavior. *Neuron* 2013;77:624–638.

28. Woo MA, Macey PM, Fonarow GC, Hamilton MA, Harper RM. Regional brain gray matter loss in heart failure. *J Appl Physiol* 2003;95:677–684.
29. Avelar WM, D'Abreu A, Coan AC, et al. Asymptomatic carotid stenosis is associated with gray and white matter damage. *Int J Stroke* 2015;10:1197–1203.
30. Lorio S, Lutti A, Kherif F, et al. Disentangling in vivo the effects of iron content and atrophy on the ageing human brain. *Neuroimage* 2014;103:280–289.
31. Braak H, Braak E. Neuropathological stageing of Alzheimer-related changes. *Acta Neuropathol* 1991;82:239–259.
32. Critchley HD, Mathias CJ, Josephs O, et al. Human cingulate cortex and autonomic control: converging neuroimaging and clinical evidence. *Brain* 2003;126:2139–2152.
33. Oppenheimer SM, Kedem G, Martin WM. Left-insular cortex lesions perturb cardiac autonomic tone in humans. *Clin Auton Res* 1996;6:131–140.
34. Krause T, Werner K, Fiebach JB, et al. Stroke in right dorsal anterior insular cortex is related to myocardial injury. *Ann Neurol* 2017;81:S02–S11.
35. Dickerson BC, Stoub TR, Shah RC, et al. Alzheimer-signature MRI biomarker predicts AD dementia in cognitively normal adults. *Neurology* 2011;76:1395–1402.
36. Allan C, Zsoldos E, Filippini N, et al. Life-time hypertension as a predictor of brain structure in older adults: a prospective cohort study. *Br J Psychiatry* 2015;206:308–315.
37. Muller M, van der Graaf Y, Visseren FL, Vlek AL, Mali WP, Geerlings MI. Blood pressure, cerebral blood flow, and brain volumes: The SMART-MR study. *J Hypertens* 2010;28:1498–1505.
38. Kennedy KM, Erickson KI, Rodrigue KM, et al. Age-related differences in regional brain volumes: a comparison of optimized voxel-based morphometry to manual volumetry. *Neurobiol Aging* 2009;30:1657–1676.
39. Tardif CL, Steele CJ, Lampe L, et al. Investigation of the confounding effects of vasculature and metabolism on computational anatomy studies. *Neuroimage* 2017;149:233–243.
40. Strong JP, Malcom GT, McMahan CA, et al. Prevalence and extent of atherosclerosis in adolescents and young adults. *JAMA* 1999;281:727–735.
41. Maillard P, Mitchell GF, Himali JJ, et al. Effects of arterial stiffness on brain integrity in young adults from the Framingham Heart Study. *Stroke* 2016;47:1030–1036.
42. Neuhauser HK, Adler C, Rosario AS, Diederichs C, Ellert U. Hypertension prevalence, awareness, treatment and control in Germany 1998 and 2008–11. *J Hum Hypertens* 2015;29:1–7.
43. Chobanian A V, Bakris GL, Black HR, et al. Seventh report of the Joint National Committee on Prevention, Detection, Evaluation, and Treatment of High Blood Pressure. *Hypertension* 2003;42:1206–1252.
44. Whelton PK, Carey RM, Aronow WS, et al. 2017 ACC/AHA/AAPA/ABC/ACPM/AGS/APhA/ASH/ASPC/NMA/PCNA guideline for the prevention, detection, evaluation, and management of high blood pressure in adults. *Hypertension* 2018;7:1269–1324.

Neurology®

Association of peripheral blood pressure with gray matter volume in 19- to 40-year-old adults

H. Lina Schaare, Shahrzad Kharabian Masouleh, Frauke Beyer, et al.

Neurology published online January 23, 2019

DOI 10.1212/WNL.0000000000006947

This information is current as of January 23, 2019

| | |
|---|---|
| Updated Information & Services | including high resolution figures, can be found at: http://n.neurology.org/content/early/2019/01/23/WNL.0000000000006947.full |
| Subspecialty Collections | This article, along with others on similar topics, appears in the following collection(s): All Cerebrovascular disease/Stroke http://n.neurology.org/cgi/collection/all_cerebrovascular_disease_stroke MRI http://n.neurology.org/cgi/collection/mri Risk factors in epidemiology http://n.neurology.org/cgi/collection/risk_factors_in_epidemiology Stroke prevention http://n.neurology.org/cgi/collection/stroke_prevention Vascular dementia http://n.neurology.org/cgi/collection/vascular_dementia |
| Permissions & Licensing | Information about reproducing this article in parts (figures, tables) or in its entirety can be found online at: http://www.neurology.org/about/about_the_journal#permissions |
| Reprints | Information about ordering reprints can be found online: http://n.neurology.org/subscribers/advertise |

Neurology® is the official journal of the American Academy of Neurology. Published continuously since 1951, it is now a weekly with 48 issues per year. Copyright © 2019 American Academy of Neurology. All rights reserved. Print ISSN: 0028-3878. Online ISSN: 1526-632X.

